

## THE NATURE OF BLUE CORES IN SPHEROIDS: A POSSIBLE CONNECTION WITH AGN AND STAR FORMATION<sup>†</sup>

FELIPE MENANTEAU<sup>1</sup>, ANDRÉ R. MARTEL<sup>1</sup>, PAOLO TOZZI<sup>2</sup>, BRENDA FRYE<sup>3</sup>, HOLLAND C. FORD<sup>1</sup>, LEOPOLDO INFANTE<sup>4</sup>, NARCISO BENÍTEZ<sup>1,5</sup>, GASPAR GALAZ<sup>4</sup>, DANIEL COE<sup>1</sup>, GARTH D. ILLINGWORTH<sup>6</sup>, GEORGE F. HARTIG<sup>7</sup> AND MARC CLAMPIN<sup>8</sup>

*Accepted for publication in the Astrophysical Journal, November 4, 2004*

### ABSTRACT

We investigate the physical nature of blue cores in early-type galaxies through the first multi-wavelength analysis of a serendipitously discovered field blue-nucleated spheroid in the background of the deep ACS/WFC *griz* multicolor observations of the cluster Abell 1689. The resolved  $g-r$ ,  $r-i$  and  $i-z$  color maps reveal a prominent blue core identifying this galaxy as a “typical” case study, exhibiting variations of 0.5–1.0 mag in color between the center and the outer regions, opposite to the expectations of reddened metallicity induced gradients in passively evolved ellipticals. From a Magellan-Clay spectrum we secure the galaxy redshift at  $z = 0.624$ . We find a strong X-ray source coincident with the spheroid galaxy. Spectral features and a high X-ray luminosity indicate the presence of an AGN in the galaxy. However, a comparison of the X-ray luminosity to a sample derived from the Chandra Deep Field South displays  $L_X$  to be comparable to Type I/QSO galaxies while the optical flux is consistent with a normal star-forming galaxy. We conclude that the galaxy’s non-thermal component dominates at high-energy wavelengths while we associate the spheroid blue light with the stellar spectrum of normal star-forming galaxies. We argue about a probable association between the presence of blue cores in spheroids and AGN activity.

*Subject headings:* galaxies: elliptical and lenticular, cD — galaxies: active — X-rays: galaxies

### 1. INTRODUCTION

Early-type galaxies have been the focal point for probing one of the main expectations from hierarchical models of galaxy formation: the continuous assembly of galaxies with redshift via mergers. Considerable attention has been devoted to field ellipticals at intermediate redshifts with high-resolution multicolor data that can provide confident morphological classification. The Hubble Deep Fields (HDFs) and more recently abundant Advanced Camera for Surveys (ACS) deep imaging has provided significant advances. Recent studies use the evolution of the fundamental plane for field ellipticals (Treu et al. 2002; van Dokkum & Ellis 2003) to constrain their evolution by comparing to cluster ellipticals, and their colors and number evolution as a function of redshift (e.g. Bell et al. 2004).

A relatively new approach is the use of color inhomogeneities exploiting the resolved colors from Hubble Space Telescope (HST) ellipticals to trace recent star formation activity (Abraham et al. 1999; Papovich et al. 2003). The studies’ chief discovery is that  $\approx 30\%$  of HST selected spheroids have internal color variations, that depart from the expectation for passively evolved ellipticals (Menanteau, Abraham, & Ellis 2001a; Menanteau et al. 2004). Moreover, in most cases the color variations mani-

fest themselves via the presence of blue cores, an effect of opposite sign to that expected from metallicity gradients on passively evolved ellipticals. Until now, blue cores in ellipticals have been solely associated with star formation attributed to differences in local potential well which makes star-formation more efficient in the central region of the galaxy (Menanteau et al. 2001b; Friaça & Terlevich 2001). However, the physical nature of these objects has been elusive as they have been only detected in extremely deep HST observations (e.g. the HDFs) and deep spectroscopic observations have been rather limited (i.e. van Dokkum & Ellis 2003) due to the long integration times required to acquire high-signal spectrum of faint ellipticals.

In this Letter, we investigate the physical origin of the blue cores in spheroids through the discovery of a blue-nucleated spheroid galaxy associated with a strong x-ray source. We use a combination of, deep ground-based spectrum, HST/ACS deep multicolor observations and archival Chandra X-ray observations to explore the probable link between AGN activity and the manifestation of blue central light in spheroids. We adopt a flat cosmology with  $h = 0.7$ ,  $\Omega_m = 0.3$  and  $\Omega_\Lambda = 0.7$  throughout.

### 2. MULTI-WAVELENGTH OBSERVATIONS

#### 2.1. Optical Imaging of Abell 1689

The ACS observations of Abell 1689 were taken in June 2002 as part of the ACS Guaranteed Time Observations (GTO) science program. They consist of deep exposures of 4, 4, 3 and 7 orbits in the F475W( $g$ ), F625W( $r$ ), F775W( $i$ ) and F850LP( $z$ ) bands, respectively. The images were aligned, cosmic-ray rejected and drizzled together into a single geometrically corrected image using APSIS (ACS Pipeline Science Investigation Software; Blakeslee et al. 2003) at Johns Hopkins University, leading to total exposures of 9500, 9500, 11800 and 16600 sec in  $g$ ,  $r$ ,  $i$  and  $z$ , respectively, and a final pixel scale of  $0''.05 \text{ pixel}^{-1}$ . We refer to Broadhurst et al. (2004) for a more detailed account of the ACS observations and photometry. Initial object detection, extraction, and in-

<sup>1</sup> Department of Physics and Astronomy, Johns Hopkins University, 3400 North Charles Street, Baltimore, MD 21218.

<sup>2</sup> INAF Osservatorio Astronomico di Trieste, via Tiepolo 11, I-34131 Trieste, Italy.

<sup>3</sup> Department of Astrophysical Sciences, Peyton Hall - Ivy Lane Princeton, NJ 08544.

<sup>4</sup> Departamento de Astronomía y Astrofísica, Pontificia Universidad Católica de Chile, Casilla 306, Santiago 22, Chile.

<sup>5</sup> Instituto de Astrofísica de Andalucía (CSIC), C/Camino Bajo de Huétor, 24, Granada, 18008, Spain.

<sup>†</sup> Based on observations obtained at Las Campanas Observatory

<sup>6</sup> UCO/Lick Observatory, University of California, Santa Cruz, CA 95064.

<sup>7</sup> STScI, 3700 San Martin Drive, Baltimore, MD 21218.

<sup>8</sup> NASA Goddard Space Flight Center, Laboratory for Astronomy and Solar Physics, Greenbelt, MD 20771.

tegrated photometry were taken from the output APSIS SE-tractor catalogs using the ACS photometric calibration in AB magnitudes. Ancillary ground-based imaging in the  $U$  band and near-infrared  $J$ ,  $H$ ,  $K$  bands matching the ACS-defined apertures were taken from the Abell 1689 catalog of Coe et al. (in preparation), which include point spread function (PSF) corrected ground-based magnitudes.

### 2.2. Deep LDSS2 Magellan Spectrum

The spectroscopic information is based on the deep multi-object observations taken with the Las Campanas Observatory Magellan-Clay 6.5m telescope on May 26, 27 and 28, 2003. We used the low-dispersion survey spectrograph 2 (LDSS2) as part of a spectroscopic survey of Abell 1689 (Frye et al. 2004). Targets for the program were selected following two criteria: 1) acquiring redshifts for the multiply-lensed galaxies discovered by Broadhurst et al. (2004), and 2) securing spectra for high redshift background galaxies. We were particularly careful to include in all our LDSS2 masks the only spheroidal galaxy with a blue core in the ACS field of Abell 1689.

We used our own IDL reduction software to handle a large number of spectra efficiently. Optimizing for background-limited data, our aim was to maximize the signal-to-noise ratio without resampling the data, so that groups of pixels carrying faint continuum signal have every chance of being detected as a coherent pattern in the final reduced image (see Frye et al. 2002 for details). The final co-added, flux-calibrated spectrum of the galaxy totaled 10h through a  $1''.0$  slit in a seeing of  $0''.6 - 0''.8$  using the Med/Blue grism at 300 lines/mm. Its wavelength dispersion is  $5\text{\AA} \text{ pixel}^{-1}$ , determined from unblended sky lines, and its spectral coverage,  $\simeq 4000 - 8500 \text{\AA}$ .

### 2.3. Chandra X-ray Observations

We investigated the AGN nature of our blue core spheroid from X-ray archival data. We used the Abell 1689 observations from the Chandra X-ray Observatory using ACIS-I in FAINT mode in two exposures of about 10.7 ks and 10.3 ks for a total of 21 ks after data reduction with the CIAO software. We smoothed out the X-ray image of pixel size  $0.984''$ , with a  $1.5\sigma$  Gaussian filter and superimposed its flux contours over the ACS image. From Fig. 1 we see two main X-ray sources within the ACS coverage of Abell 1689, the strongest coming from the central cD galaxy in Abell 1689 (Xue & Wu 2002) and on the upper right of the ACS image a strong X-ray source which we positively associate with the blue core spheroid in our study.

We also considered the possibility of radio sources being associated with the object. Based on radio wavelength archival data from the VLA FIRST radio survey (White et al. 1997), we found no radio counterpart associated with the blue core galaxy at the flux limits of the survey ( $0.97 \text{ mJy/beam}$ ).

## 3. ANALYSIS

To search for color variations in spheroids, we examine galaxies in the ACS field of Abell 1689 via the construction of  $g-r$ ,  $r-i$ , and  $i-z$  color maps for all 742 galaxies with  $i_{775w} < 24.5$ . Although the effective area for this search is rather limited due to the presence of the cluster itself and the gravitational lens magnification, we successfully located one background spheroidal in one of the corners of the ACS field-of-view with a strong central blue spot similarly to those reported previously (see upper panel Fig. 2). This is the only

spheroid with a blue core in the field, including all the objects associated with the cluster. To study the color maps and galaxy profiles, we first removed the dependence of the PSF structure on wavelength by deconvolving the galaxy image in each bandpass with an appropriate PSF using the IRAF *lucy* task with flux conservation. The PSFs were derived from several observations of a well-exposed star in ACS calibration programs. The restored images were then convolved identically with the F625W PSF, thus removing any color dependence due to the PSF shape. We used this images to create the galaxy resolved color maps. These show a prominent blue core with color differences of  $\simeq 1.0 \text{ mag}$  in  $g-r$ ,  $\simeq 0.8 \text{ mag}$  in  $r-i$  and  $\simeq 0.9$  in  $i-z$ .

We verified if the galaxy possesses an unresolved nucleus, a common signature of nuclear activity, by comparing its nuclear profile in each filter with that of an observed PSF. The galaxy radial profiles were extracted with the IRAF *radprof* task with “background” subtraction defined in an annulus of radius 6 pixels ( $0''.3$ ) and width 2 pixels, located inside the host galaxy. The resulting galactic profiles were then compared with those of the PSF star. A positive point source identification was ascertained in all four filters out to a radius of 5 pixels ( $0''.25$ ). The match of the galaxy’s nuclear profile with the PSF is best in F475W filter, where the host galaxy contamination is the least. The F625W profiles exhibit the largest deviation possibly from contamination by  $[\text{O II}]\lambda 3727$  line emission (see Fig. 2).

The spectrum (Fig. 2) shows prominent emission lines that indicate the presence of an active nucleus and also suggest star formation activity. The galaxy contains the distinctive Mg II, H $\beta$  and  $[\text{O III}]\lambda\lambda 4959, 5007$  nebular lines associated with AGNs. However, the signal is not high enough to see the broad-line component for the Mg II and H $\beta$  permitted lines, and H $\alpha$  lies outside the observed spectral range. The continuum does not follow a pure power-law, but rather includes some absorption features such as Mgb.

Additional information confirming the presence of an active nucleus comes from the X-ray observations. The galaxy is detected as a point source in the X-ray with a very high signal and with a total of  $\simeq 130$  net counts in the 0.3–10 keV band, extracted from a circular region of  $8''$ . From a difference of almost 9 months between the two Chandra observations, the source seems to be variable with a luminosity decrease of  $\sim 30\%$  at a 2 sigma c.l. in the soft band (0.5–2 keV). However, we do not detect any variability in the hard band. This is expected, since variability is routinely found in X-ray sources in Chandra surveys (Paolillo et al. 2004). To correct for possible contamination from the diffuse emission from the cluster, which is very strong in the position of the galaxy image, we experimented extracting three different backgrounds around the galaxy and determined that the background is not affecting our results significantly. Due to the low number of net detected counts, we used the Cash (1979) statistics to fit the spectrum of the galaxy with XSPEC (V11.3) the energy range 0.6–8 keV, to avoid calibration uncertainties at energies lower than 0.6 keV. Our model is a simple power-law plus a Galactic absorption and an intrinsic absorption. We find a spectral slope of  $\Gamma = 1.5 \pm 0.2$  and an upper limit to the intrinsic absorption of  $2 \times 10^{21} \text{ cm}^{-2}$ . The redshift is frozen to  $z = 0.624$  and the Galactic absorption to  $N_H = 1.82 \times 10^{20} \text{ cm}^{-2}$ . The luminosity in the rest-frame 0.5–2 keV and 0.5–10 keV band is  $L_X = 2.95 \times 10^{43} \text{ erg s}^{-1}$  and  $L_X = 1.04 \times 10^{44} \text{ erg s}^{-1}$  respectively (see Table 1). Both the absence of significant absorption and the high lumi-

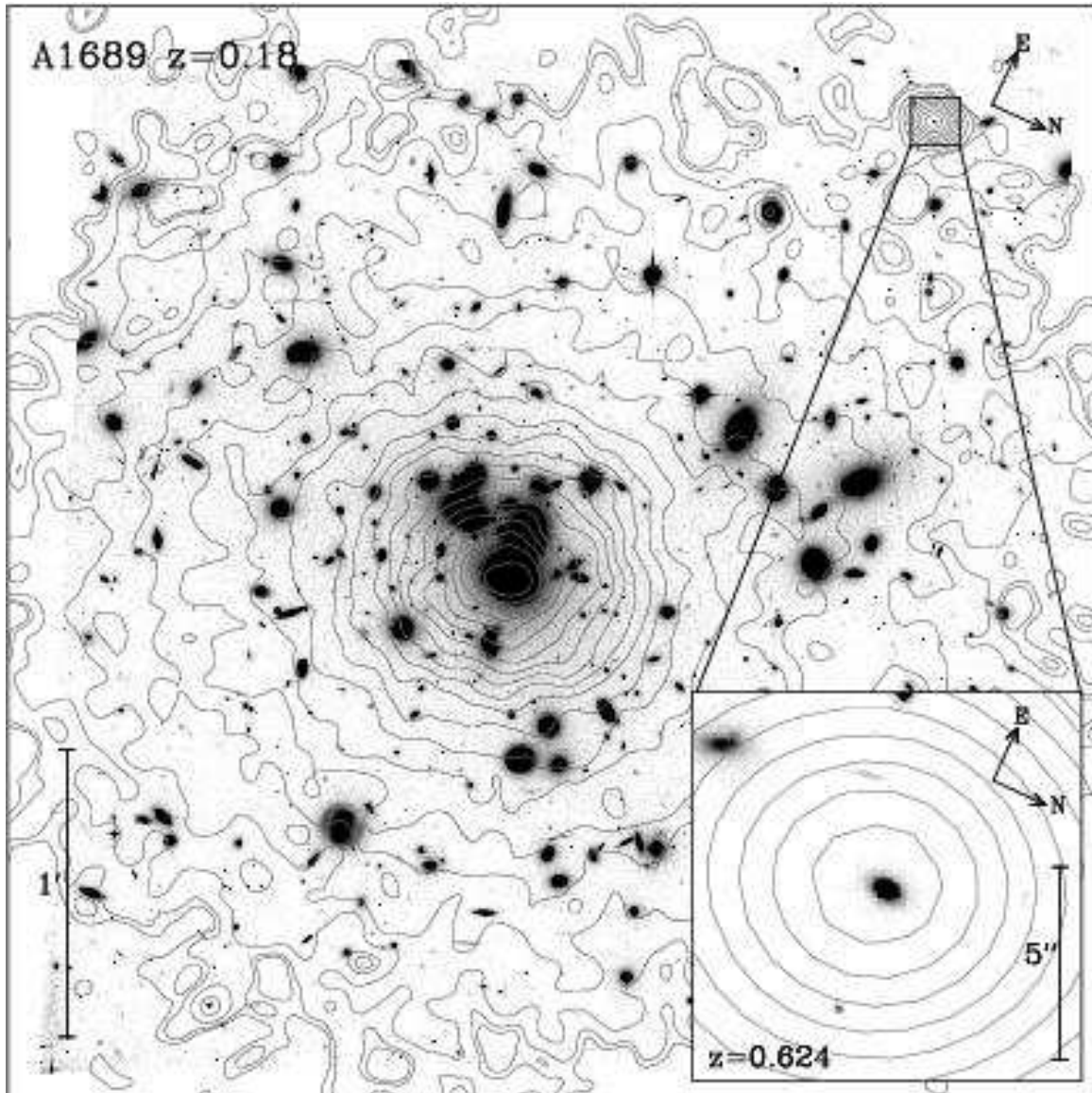


FIG. 1.— The ACS/WFC imaging of Abell 1689 ( $z = 0.18$ ) with the superimposed Chandra 0.5–7 keV X-ray contour maps, consisting of 20 contours between  $\sim 0.1$ –14 counts per pixel displayed with a sqrt scale. The inset panel shows an enlargement of the background spheroid at  $z = 0.624$ , the strongest field X-ray source in the ACS field besides the cluster itself.

TABLE 1  
MULTIWAVELENGTH INFORMATION

RA	(J2000) DEC	U	F475W	F625W	AB magnitude		J	H	K	[O II]	EW( $\text{\AA}$ ) [O III]	H $\beta$	$L_{X(0.5-2 \text{ keV})}$	$L_{X(0.5-10 \text{ keV})}$
13:11:37.69	-01:19:49.8	21.60	22.07	21.92	21.39	21.27	20.69	20.44	20.04	23.5	70.7	9.68	$2.95 \times 10^{43}$	$1.04 \times 10^{44}$

nosity point towards a Type I AGN.

We also notice a residual around 4 keV, which is the observing frame energy expected for a possible Fe line complex at the rest-frame energy of  $\sim 6.4$  keV. Therefore, we repeated the fits by adding a simple Gaussian line and leaving free the energy, the width and normalization of the line. We obtain the best fit values:  $E_{line} = 3.93 \pm 0.08$  keV, and equivalent width  $EW = 0.9 \pm 0.5$  keV. In addition, the best fit slope of the power law is  $\Gamma = 1.65 \pm 0.25$ , while the upper limits on the intrinsic

absorption are somewhat larger but consistent with the values obtained without the line. The decrease in C-statistics with respect to the model without the line is  $\Delta C \sim 5.9$ . Considering that we added three free parameters defining the line, such a decrement correspond to a significance level of about 90%. However, since the best-fit energy of the line is what we expected for the redshifted 6.4 keV K-shell transition from Fe, the significance of the detected line is more than 2 sigma. We conclude that we possibly detected a Fe line originated in the

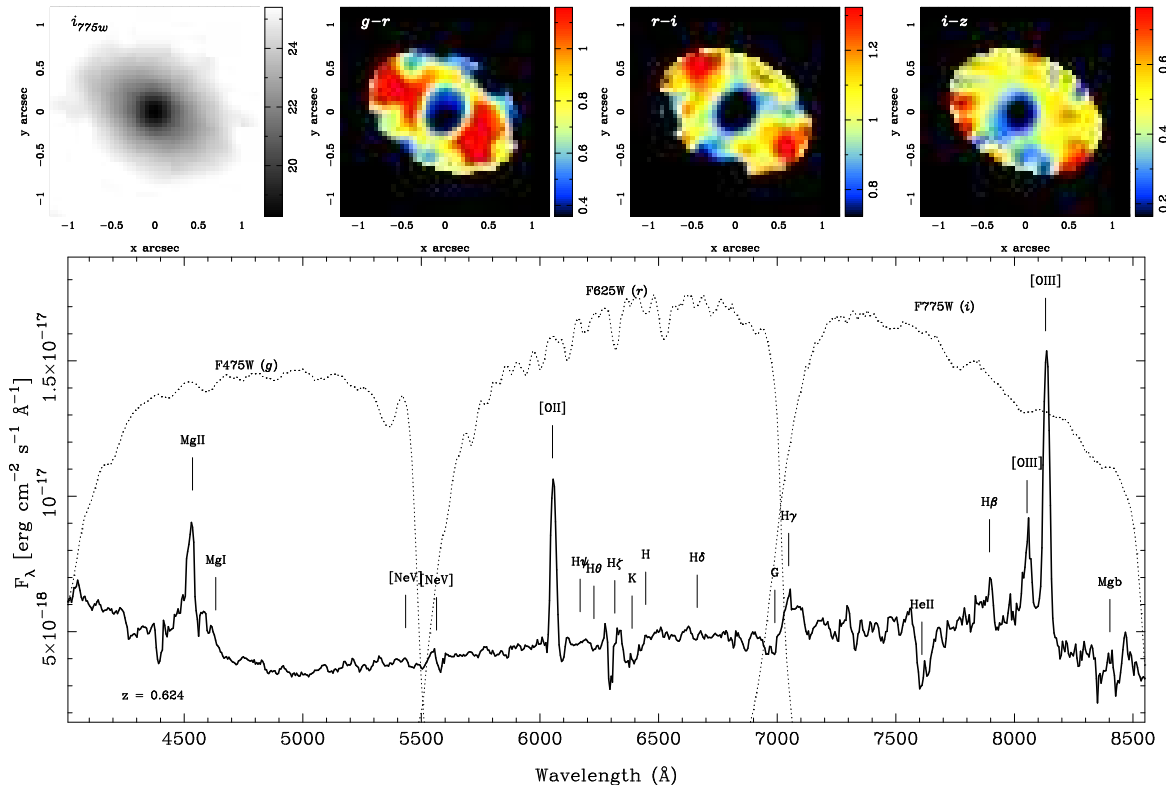


FIG. 2.— Upper panel: the  $i$ -band surface brightness and the  $g-r$ ,  $r-i$  and  $i-z$  color maps for the blue core spheroid from the ACS imaging. The figure is color coded to its real color in AB magnitudes. Lower panel: the LDSS2 observed spectrum for the galaxy at  $z = 0.624$  is shown as a solid line. The corresponding ACS filter bandpasses are shown in arbitrary units as dotted lines. Prominent spectral lines are labeled.

nuclear region, an occurrence to be verified with further observations already scheduled for A1689 (public release March 2005).

#### 4. DISCUSSION

We examine the relationship between the X-ray and optical luminosities of the galaxy and its connection with galaxy types. We compare the galaxy  $L_{X(0.2-10)}$  keV luminosity and  $K$ -band absolute AB magnitude with the galaxies in the Szokoly et al. (2004) Chandra Deep Field South (CDF-S) catalog of X-ray sources. The  $K$  absolute magnitude is computed using the  $k$ -correction derived from the Type I spectral energy distribution (SED) of the Chatzichristou (private communication) library of SEDs. In Fig. 3 (upper panel), we compare  $L_X$  and  $K$  for the galaxy (solid star) and the CDF-S sample. It is interesting to note that the galaxy has an X-ray luminosity in the same range as low luminosity QSOs (squares) and Type I AGNs (filled circles). However, the galaxy's  $K$  flux is more similar to that of Type II AGNs (open circles) or normal galaxies (triangles). This suggests that the galaxy's non-thermal component is very strong and dominant for high-energy wavelengths while there is a star-forming stellar component that contributes most of the light at optical wavelengths.

We also investigate the relation between the line flux ratios  $[O II]\lambda 3727/H\beta$  and  $\text{O}5007/H\beta$ . This diagnostic diagram has been used for the spectral classification of emission-line galaxies (see Tresse et al. 1996). In Fig. 3 (lower panel), we compare the line fluxes between the spheroid galaxy (solid star) and the values for different galaxy types taken from the spectrophotometric catalog of galaxies of Terlevich et al. (1991). We find that the galaxy has  $[O II]\lambda 3727/H\beta$  values in the same range as Type II AGNs and HII galax-

ies and that its  $\text{O}5007/H\beta$  flux is more similar to HII and normal galaxies. Moreover, the typical  $\text{O}5007/H\beta$  and  $[O II]\lambda 3727/H\beta$  values of Type I AGNs (solid circles) are significantly lower than the values of the galaxy. We consider this as further evidence for the dual nature of the galaxy. Although the spectrum shows AGN signatures such as  $MgII$  and  $[O III]\lambda 4959,5007$ , the strength of the  $[O II]\lambda 3727$  line suggest the presence of ongoing stellar formation processes. If we associate the  $[O II]\lambda 3727$  flux to stellar activity we can make a rough estimate of the galaxy star formation rate (SFR) based on its  $[O II]\lambda 3727$  luminosity,  $L[O II]$ , using the prescription of Kennicutt (1998). Whereas the rates derived from  $[O II]\lambda 3727$  are less precise than those from  $H\alpha$  due to uncertainties in the assumed  $H\alpha$  extinction, it is still possible to obtain a reasonable estimate for the galaxy SFR. We compute  $L[O II] = 2.79 \times 10^{41}$  ergs  $s^{-1}$  which yields a  $SFR = 3.90 \pm 1.12 M_{\odot} yr^{-1}$ . This represents a modest rate, lower than in massive starburst galaxies (Ranalli et al. 2003; Gilfanov et al. 2004). However it is consistent with normal disk galaxies and SFR computed for spheroids with similar blue cores, based purely on models (Menanteau et al. 2001a,b).

The  $L_{X(0.5-2 \text{ keV})}$  has been employed as a SFR indicator (see Ranalli et al. 2003; Cohen 2003), because of its link to X-ray binaries, (Persic et al. 2004), young supernova remnants and galactic winds associated to star-forming galaxies. Additionally Gilfanov et al. (2004) have derived the relation between  $L_{X(0.2-10 \text{ keV})}$  and SFR, consistent with Ranalli et al. (2003) except for low SFR (Grimm et al. 2003). Could the observed spheroid  $L_X$  be solely associated with star formation? It is hard to rule out that a fraction of it is not related, however

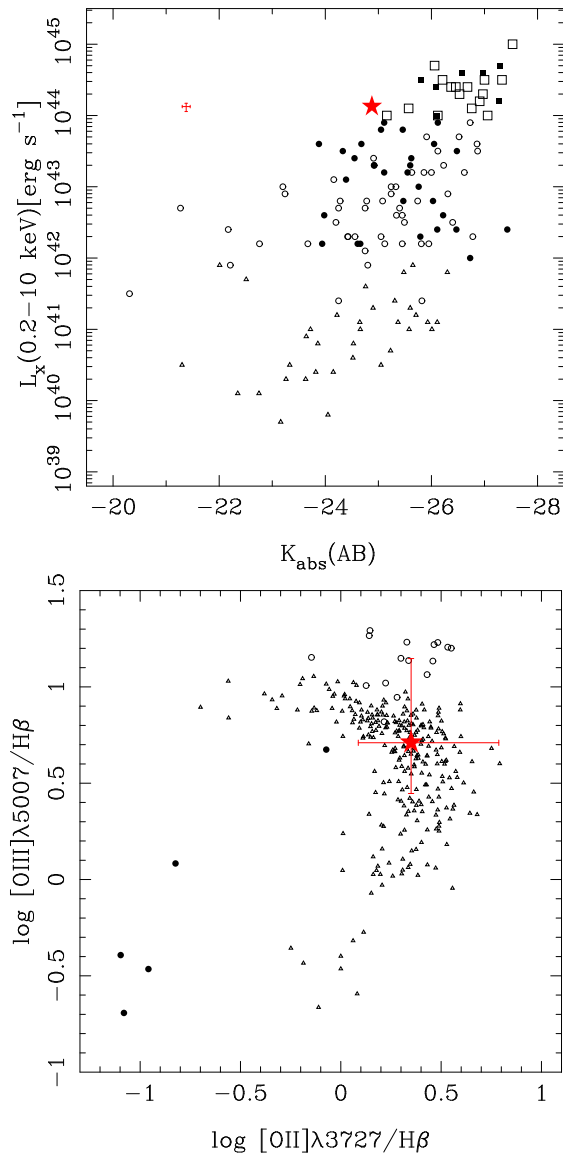


FIG. 3.— Top panel: the X-ray to optical luminosity for the Chandra Deep Field South spectroscopic catalog from Szokoly et al. (2004) compared to the spheroid galaxy. The error bars for the galaxy have been shifted to avoid overlapping with the symbol. Bottom panel: the  $[\text{O III}]\lambda 5007/\text{H}\beta$  relative to  $\text{H}\beta$  flux from the spectro-photometric catalog from Terlevich et al. (1991) compared to the values extracted for the spheroid. In both panels the red star represents the blue core spheroid; filled and open circles show Type I and Type II AGNs respectively, squares represent QSO galaxies and open triangles normal and HII galaxies.

the 2–10 keV hard band luminosity  $L_X = 7.5 \times 10^{43} \text{ erg s}^{-1}$ , would suggest an extremely high SFR ( $> 10^4 \text{ M}_\odot \text{ yr}^{-1}$ ) in contradiction with the optical data suggestive of low star-formation activity. There is also a tight correlation between  $L(1.4 \text{ GHz})$  radio luminosity and  $L_X$  for starburst galaxies (Cohen 2003). However, we report no signal for the galaxy at radio wavelengths (i.e. § 2).

## 5. CONCLUSION

Based on the galaxy’s spectral features and its X-ray luminosity, we have determined the presence of an active non-thermal component in the blue spheroid galaxy identified in the background field of Abell 1689. Star formation and AGNs have been suggested to be closely inter-connected (Levenson et al. 2001). However, they have been related mostly with Seyfert 2 galaxies which are heavily absorbed in their hard X-ray emission—not the case for this galaxy. Moreover, the fact that we observe such a prominent blue core in the ACS images suggests that the central region is not particularly affected by dust obscuration, nor that it contains a dusty enshrouded starburst. On the other hand most present-day galaxies harbor supermassive black holes, which may have an important role in the formation of ellipticals and bulges (Merritt & Ferrarese 2001). It is tantalizing to relate the galaxy central blue light with the rapid mass infall into a central black hole which might trigger star formation, and the subsequent fueling of gas into the AGN which might be the phenomenon we are observing.

The advent of wide areas with deep publicly available HST/ACS multicolor imaging and Chandra X-ray observations will make it possible to examine whether the association between AGNs and blue core spheroids is a common feature or just a rare occurrence. If they prove to be a constant feature in blue core spheroids, these might represent a new galaxy subclass and may provide evidence for a more delayed formation scenario for early-type galaxies.

We thank Ann Hornschemeier for useful conversations on the subject. ACS was developed under NASA contract NAS 5-32865, and this research is supported by NASA grant NAG5-7697. LI and GG acknowledge support from FONDAP “Center for Astrophysics”.

## REFERENCES

- Abraham, R. G., Ellis, R. S., Fabian, A. C., Tanvir, N. R., & Glazebrook, K. 1999, *MNRAS*, 303, 641  
 Bell, E. F. et al. 2004, *ApJ*, 600, L11  
 Blakeslee, J. P., Anderson, K. R., Meurer, G. R., Benítez, N., & Magee, D. 2003, in *Astronomical Data Analysis Software and Systems XII ASP Conference Series*, Vol. 295, 2003 H. E. Payne, R. I. Jedrzejewski, and R. N. Hook, eds., p.257, 257+  
 Broadhurst, T. et al. 2004, *ApJ* submitted  
 Cash, W. 1979, *ApJ*, 228, 939  
 Cohen, J. G. 2003, *ApJ*, 598, 288  
 Friaça, A. C. S., & Terlevich, R. J. 2001, *MNRAS*, 325, 335  
 Frye, B., Broadhurst, T., & Benítez, N. 2002, *ApJ*, 568, 558  
 Gilfanov, M., Grimm, H.-J., & Sunyaev, R. 2004, *MNRAS*, 347, L57  
 Grimm, H.-J., Gilfanov, M., & Sunyaev, R. 2003, *MNRAS*, 339, 793  
 Kennicutt, R. C. 1998, *ARA&A*, 36, 189  
 Levenson, N. A., Weaver, K. A., & Heckman, T. M. 2001, *ApJ*, 550, 230  
 Menanteau, F., Abraham, R. G., & Ellis, R. S. 2001a, *MNRAS*, 322, 1  
 Menanteau, F. et al. 2004, *ApJ*, 612, xxx  
 Menanteau, F., Jimenez, R., & Matteucci, F. 2001b, *ApJ*, 562, L23  
 Merritt, D., & Ferrarese, L. 2001, *MNRAS*, 320, L30  
 Paolillo, M., Schreier, E. J., Giacconi, R., Koekemoer, A. M., & Grogin, N. A. 2004, *ApJ*, 611, 93  
 Papovich, C., Giavalisco, M., Dickinson, M., Conselice, C. J., & Ferguson, H. C. 2003, *ApJ*, 598, 827  
 Persic, M., Rephaeli, Y., Braitto, V., Cappi, M., Della Ceca, R., Franceschini, A., & Gruber, D. E. 2004, *A&A*, 419, 849  
 Ranalli, P., Comastri, A., & Setti, G. 2003, *A&A*, 399, 39  
 Szokoly, G. P. et al. 2004, *ApJS* (astro-ph/0312324)  
 Terlevich, R., Melnick, J., Masegosa, J., Moles, M., & Copetti, M. V. F. 1991, *A&AS*, 91, 285  
 Tresse, L., Rola, C., Hammer, F., Stasinska, G., Le Fevre, O., Lilly, S. J., & Crampton, D. 1996, *MNRAS*, 281, 847  
 Treu, T., Stiavelli, M., Casertano, S., Møller, P., & Bertin, G. 2002, *ApJ*, 564, L13

van Dokkum, P. G., & Ellis, R. S. 2003, *ApJ*, 592, L53

Xue, S., & Wu, X. 2002, *ApJ*, 576, 152

White, R. L., Becker, R. H., Helfand, D. J., & Gregg, M. D. 1997, *ApJ*, 475,  
479